ACCSCIENCE PUBLISHING

International Journal of Bioprinting

RESEARCH ARTICLE

Manipulating fungal growth in engineered living materials through precise deposition of nutrients

Jia Heng Teoh[1], Eugene Soh[1], and Hortense Le Ferrand[1,2,3,4,*]

[1]School of Mechanical and Aerospace Engineering, Nanyang Technological University, Singapore

[2]School of Materials Science and Engineering, Nanyang Technological University, Singapore

[3]Singapore Center for 3D Printing, Nanyang Technological University, Singapore

[4]Future Cities Laboratory, Singapore ETH Centre, Singapore

Abstract

One main challenge of emerging fungal-based engineered living materials (ELMs) lies in achieving localized multi-material properties in these structures. Although three-dimensional (3D) printing can efficiently vary local composition and properties, it has not yet been demonstrated in fungal-based ELMs. This work thus explores the concept of using nutrients to manipulate fungal foraging behavior in 3D structures fabricated using direct ink writing (DIW) for the next generation of fungal-based ELMs. Using two fungal strains (*Pleurotus ostreatus* and *Ganoderma lucidum*), this study showed that the ink formulation used is suitable for both DIW and mycelium growth. Varying the nutrient content allows for either the inhibition or promotion of exploration and bridging of mycelium in different sections, the control of mycelium density in three dimensions and the fabrication of patterned surfaces. There is potential in fabricating patterned fungal-based ELMs and lab-on-a-chip systems to investigate the effects of other substances and microorganisms on the foraging behavior of mycelium.

Keywords: 3D printing; Direct ink writing; Engineered living material; Mycelium; Hydrogel; Foraging behavior

***Corresponding author:**
Hortense Le Ferrand
(hortense@ntu.edu.sg)

Citation: Teoh JH, Soh E, Le Ferrand H. Manipulating fungal growth in engineered living materials through precise deposition of nutrients. *Int J Bioprint*. 2024. doi: 10.36922/ijb.3939

Received: June 14, 2024
Revised: July 18, 2024
Accepted: July 27, 2024
Published Online: July 30, 2024

1. Introduction

Engineered living materials (ELMs) are an emerging type of biomaterials that utilizes living cells to give functionalities to an otherwise inanimate material.[1–3] Among other cells, fungal-based ELMs—which incorporate filamentous fungus that form a three-dimensional (3D) net of fungal cells called mycelium—have demonstrated interesting properties leading to potential applications such as self-healing textiles,[4–6] living structures,[7] or robotics.[8] In designing fungal-based ELMs, it is important to ensure that the fungus is growing effectively throughout the structure with the desired mycelium density. Mycelium is known to grow a uniform fungal skin on the exterior of the structure at the material–air interface, whereas the center of the structure is usually devoid of mycelium due to positive aerotropism.[9,10] Being able to control the growth of mycelium in materials is instrumental for tailoring the mechanical properties of the structure, in particular its stiffness.[10] Furthermore, for ELMs to function as living

machines, they may need to also be compartmentalized with various properties and functions within one ELM, calling for material heterogeneity and localized growth of cells. There is therefore a need to be able to control the growth and location of mycelium on materials to enable production of new types of ELMs.

A common method to create localized properties in a material is to use multi-material 3D printing. By using methods including fused deposition modeling (FDM) and direct ink writing (DIW), materials such as plastics and hydrogels can be precisely positioned in a 3D space, allowing for the fabrication of complex structures.[11,12] With multiple nozzles, additional materials and compositions can be incorporated into the same process, allowing for the fabrication of a multi-material structure.[13–15] The utilization of 3D printing in fungal-based ELMs with variations in material, mycelium inoculation techniques, and scale has been gaining traction. For example, direct inoculation involves the addition of mycelium into the ink prior to the fabrication of the structure.[8,16–18] As for indirect inoculation, the structure is first printed before it is placed in direct contact with separately cultured fungi. The fungi then grow toward the structure, eventually enveloping it in the process.[19,20] However, the use of multiple nozzles in fabricating complex, multi-material fungal-based ELMs has yet to be explored. On the contrary, it is generally found that mycelium materials grow a homogeneous fungal skin on their surface that prevents local tailoring of their properties. Exploring ways to create multi-material types of fungal-based ELMs are thus needed.

In nature, organisms have developed various growth, foraging, or translocation strategies to survive in ecosystems that may not provide continuous supply of nutrients.[21] When faced with an environment that is either abundant or lacking in nutrients, filamentous fungi tend to exhibit two main foraging behaviors: phalanx and guerrilla.[22,23] Phalanx, also known as exploitative growth, is characterized by a slow extension rate of hyphae and high mycelium density. Guerrilla, also known as explorative growth, is characterized by a fast extension rate of hyphae, which are the single filaments in the mycelium network, but a low mycelium density. In a low-nutrient environment, guerrilla is the dominant growth pattern whereas phalanx is usually observed when the fungus is in a high-nutrient environment.[8,22,24,25] Fungi are able to switch between these foraging behaviors depending on the environment they encounter.[26,27] While available nutrients do dictate the type of growth behavior, the degree to which fungi explore or exploit their environment also depends on the species.[22,28,29] In a similar environment, species such as *Coprinus angulatus* and *Psilocybe* cf. *subviscida* may exhibit guerrilla-type behavior in terms of being fast growers and long-range foragers while others such as *Tricholomella constricta* and *Leucopaxillus genetianeus* exhibit phalanx-type behavior as they have the tendency to grow slowly and branch profusely.[22] These species and nutrient-dependent variations in mycelium morphology could therefore be used to tailor the local distribution and morphology of mycelium for future fungal-based ELMs.

In this work, we investigated the growth of mycelium from two fungal species *Ganoderma lucidum* (*G. lucidum*, Lingzhi mushroom) and *Pleurotus ostreatus* (*P. ostreatus*, oyster mushroom) in 3D-printed structures containing local variations of nutrient content. More specifically, mycelium-containing inks were developed with varying concentrations of malt and peptone as growth media. These inks were then precisely locally deposited using DIW. The control and tailoring of the mycelium density, growth behavior over acellular gaps containing different levels of nutrients, and mycelium growth in various directions were demonstrated. Finally, intentionally patterned structures were fabricated as proof-of-concept examples of what this approach can achieve. While fundamental, this work can be leveraged to create more complex types of fungal-based ELMs to manipulate properties such as self-healing capabilities and to explore new applications.

2. Materials and methods

2.1. Materials

The following items were purchased from Sigma Aldrich (USA): malt, peptone, agar, carboxymethyl cellulose (CMC), sodium alginate, calcium chloride, and gentamicin sulfate. *P. ostreatus* spawn bags were obtained from Bewilder (Singapore), whereas *G. lucidum* was acquired from Malaysian Feedmills Farms (Malaysia).

2.2. Mycelium culture

In this study, mycelium was cultured on both solid agar substrates and in liquid cultures. For solid agar substrates, malt agar plates were made by dissolving agar (2.5% w/v), malt (2.0% w/v), and peptone (0.1% w/v) in deionized water. The mixture was then autoclaved (Hiclave HG 80, Hirayama, Japan) at 121°C for 20 min and poured into 90 mm Petri dishes. The mixture was allowed to cool and set before they were inoculated with a solid agar plug of 9 mm diameter containing mycelium from a previously inoculated plate. For liquid mycelium cultures, malt broth was made by dissolving malt (1.7% w/v) and peptone (0.3% w/v) in deionized water and was autoclaved at 121°C for 20 min. After cooling, the broth was supplemented with gentamicin sulfate (50 μg/mL), followed by the addition of a solid agar plug containing mycelium. Liquid mycelium cultures were then left to grow under constant magnetic

stirring for 7–10 days before they were used for subsequent experiments.

2.3. Effect of malt and peptone on mycelium growth

A two-level full factorial design of experiment was adopted to study the effect of malt and peptone on mycelium growth. Malt agar plates were made as described above, except that the malt and peptone concentrations were varied at two different levels, as shown in **Table 1**. The growth of mycelium on each set was monitored over 14 days. Digital images of the agar plates were taken and processed using ImageJ,[30] and the growth rate was quantified by measuring the area of mycelium on each set over 14 days. To determine the dry weight of biomass produced, the mycelium films were peeled from each agar plate after 14 days of culture. They were then dried in an oven at 50°C for 3 days before they were subsequently weighed. Triplicates were analyzed to ensure reproducibility of results.

2.4. Inks preparation for 3D printing

The inks for DIW were made by dissolving alginate (1.2% w/v) and CMC (3.6% w/v) in a solution of malt and peptone at 45°C. The concentration of malt and peptone was adjusted according to Table 1. In addition, another set of inks that would be mixed with liquid mycelium was made using malt (2% w/v) and peptone (0.1% w/v) and were denoted as the medium level of both malt and peptone, respectively. The inks were stirred using a magnetic stirrer until all the alginate and CMC had completely dissolved. Agar (3% w/v) was then added, and the temperature was increased to facilitate the dissolution of agar. The mixture was then autoclaved at 121°C for 20 min, and once removed from the autoclave, it was stirred until it had set. Liquid mycelium was then mixed into the ink at a ratio of 1:5 (v/v) and was stirred until a fine paste was formed. For acellular inks, malt and peptone broths of the corresponding malt and peptone concentrations, respectively, that were devoid of mycelium were added instead at the same volumetric ratio.

2.5. Rheology

The rheological properties of the inks were evaluated using a Bohlin Gemini HR Nano rheometer (Malvern, UK). A 15 mm serrated plate and a measuring gap of 0.5 mm were used. Samples were pre-sheared using a shear rate of 10 s^{-1} for 30 s before being allowed to equilibrate for 60 s. For steady-state viscosity tests, a shear rate range of 0.01–1000 s^{-1} was used. The viscosity as a function of shear rate was then recorded. For amplitude sweep tests, using a frequency of 0.5 Hz, the shear stress was increased from 0.1 to 500 Pa. The storage and loss moduli were recorded. All samples were tested at 25°C. Triplicates of each sample were analyzed.

Table 1. Concentrations of malt and peptone associated with high and low levels, respectively, as used in the two-level full factorial design of experiment

Nutrient component	Concentration (% [w/v])	
	Low level (−1)	High level (+1)
Malt	0.1	5
Peptone	0.01	1

2.6. 3D printing of multi-material constructs

3D-printed constructs were fabricated using DIW with an Allevi 2 bioprinter (3D Systems, USA). The structures were designed using FreeCAD and the gcode files were generated using PrusaSlicer. The inks were loaded into a 10 mL syringe (BD, USA). 22G tapered nozzles (Nordson, USA) were used. Pneumatic pressure ranging from 20 to 30 psi was applied along with a print speed of 20 mm/s. After printing, constructs were sprayed with a solution of deionized water containing calcium chloride (3% w/v) supplemented with gentamicin sulfate (50 μg/mL) to crosslink the alginate. The growth of mycelium on the multi-material constructs was recorded over a period of 10 days. Triplicates of each design were printed and observed.

2.7. Scanning electron microscopy

The microstructure of pure mycelium sheets and fabricated fungal-based ELMs were imaged by means of scanning electron microscopy (SEM; JEOL-5600LV, Japan) on square samples each with a length of roughly 5 mm. Prior to imaging via SEM, all samples were placed in a −20°C fridge overnight and subsequently lyophilized for 24 h. Samples were cut into small pieces and mounted onto the SEM stage using carbon tape. All samples were coated with gold for 75 s at 15 mA, which is equivalent to about 11 nm coating thickness. For the SEM, an acceleration voltage of 10 kV was used. SEM images were processed using ImageJ to measure the surface porosity and hyphae diameter. The surface porosity was calculated by obtaining the average of the percentage of areas occupied by pores in the electron micrograph at three random points of each sample. The hyphae diameter was obtained by measuring the projected width of hyphae at 15 different points in an electron micrograph of the sample.

2.8. Statistical analysis

Statistical analysis was conducted using Microsoft Excel. A two-way analysis of variance (ANOVA) with a significance level of 0.05, followed by a post hoc Tukey's HSD test, was performed for data comparison. Data are presented as mean ± standard deviation.

3. Results and discussion

3.1. Ink formulation and 3D printing strategies for fungal-based ELMs

To enable the 3D printing via DIW of aqueous inks containing fungal cells to create ELMs, it is important to first design an ink system that simultaneously allows the safe growth of the fungi and satisfies the 3D printing requirements. The ink should therefore contain the nutrients necessary for the fungus to grow and develop its mycelium while the ink should also exhibit the rheological properties necessary for their extrusion through the nozzle and their shape retention after 3D printing (Figure 1). *G. lucidum* and *P. ostreatus* were two fungal species selected for this investigation, owing to their extensive use in the fabrication of mycelium-bound composites and fungal-based ELMs,[31] and their availability. Indeed, *G. lucidum* is known for its medicinal properties in traditional Chinese medicine and *P. ostreatus* is a popular mushroom used in various cuisines.

The ink for producing the fungal-based ELMs was formulated to contain agar, alginate, and CMC (Figure 1A). Agar is a polysaccharide known to be suitable for fungal growth.[32] For this ink, it provides necessary stiffness and strength for achieving the desired rheological properties of the ink. As the ink cannot be printed at elevated temperatures owing to the presence of mycelium in the ink during printing,[33,34] the agar was present as solid gel particulates, which tend to form discontinuous filaments when extruded.[17] To remedy this, CMC was added to act as a rheological modifier, allowing for a smooth extrusion of the ink at room temperature (see Supplementary File, Figure S1). Alginate was also supplemented to act as a crosslinking agent that undergoes gelation in the presence of calcium chloride.[35,36] After printing, calcium chloride solution was sprayed onto the construct to fix the printed shape to prevent sagging or deformation until the mycelium fully colonized the structure. Conveniently, the calcium ions from calcium chloride have also been reported in the literature to stimulate mycelium growth,[37] which provides an additional benefit to the process. The moisture from the calcium chloride spray also helped provide a moist environment for mycelium growth and gentamicin was incorporated into the spray to prevent contamination before the mycelium was fully grown. This is especially beneficial when the structure is printed in a non-sterile environment, away from biosafety cabinets, as conducted in this work. The ratio of each component was tailored based on each component's contribution to the rheology of the overall ink. Agar had the greatest contribution to the viscosity and rigidity of the ink, followed by CMC. While alginate was essential as the crosslinking agent, it had the least contribution to the rheology of the ink and its addition also decreased the rigidity of the overall ink (see Figures S2–S4, Supporting Information). Thus, high concentrations of agar and CMC were incorporated to provide the bulk of the viscosity and rigidity of the ink while sufficient alginate was added to enable the structure to be rigid after printing and crosslinking using calcium chloride.

The composite inks exhibited a shear-thinning behavior, which made them suitable for 3D printing via DIW (Figure 1B). The viscosity profile of the ink was also independent of the concentration of malt and peptone incorporated. As such, the printing parameters did not need to be adjusted when modifying the concentration of malt and peptone, which made it convenient for multi-material 3D printing. Furthermore, the inks had solid-like properties as the storage modulus was greater than the loss modulus ($G' > G''$) in the linear viscoelastic region for all inks (Figure 1C). Therefore, the inks did not spontaneously flow under the influence of gravity after the printing process, allowing for buildability and high shape fidelity. Indeed, various well-defined shapes could be printed using the finalized ink compositions (see Figure S5, Supporting Information).

The 3D-printed structures can be inoculated with mycelium either before the printing process (i.e., mycelium spawn or liquid culture is incorporated into the ink before printing)[8,16–18,38] or after printing (i.e., mycelium spawn is embedded into the 3D-printed structure or the structure is placed in direct contact with mycelium that was cultured separately).[19,39] In this study, the ink was inoculated directly with the liquid mycelium culture being incorporated into the ink. Compared to direct inoculation using solid spawns, the risk of clogging was lower when using the liquid culture (due to the heterogeneity of the ink caused by the added spawns), and the homogeneity of the ink was maintained. This is especially important in this study as a 22G nozzle (0.41 mm internal diameter) was used. Based on Figure 1D, the ink containing medium levels of malt and peptone can effectively support the growth of both *P. ostreatus* and *G. lucidum*. After 4 days, white, fluffy spots were seen at various parts of the surface of the structure as the mycelium began to grow. The mycelium then eventually enveloped the entire surface of the structure. These preliminary experiments that were meant to demonstrate the 3D printing of the inks have already revealed the different growth or foraging behaviors from the two fungi.

Indeed, *P. ostreatus* had a greater tendency to form hyphae that spread away from the structure and extend into the air once the surface was fully covered by the mycelium. The lack of any specific direction in the tip extension of the hyphae resulted in the underlying structure being less pronounced after the mycelium had completely enveloped

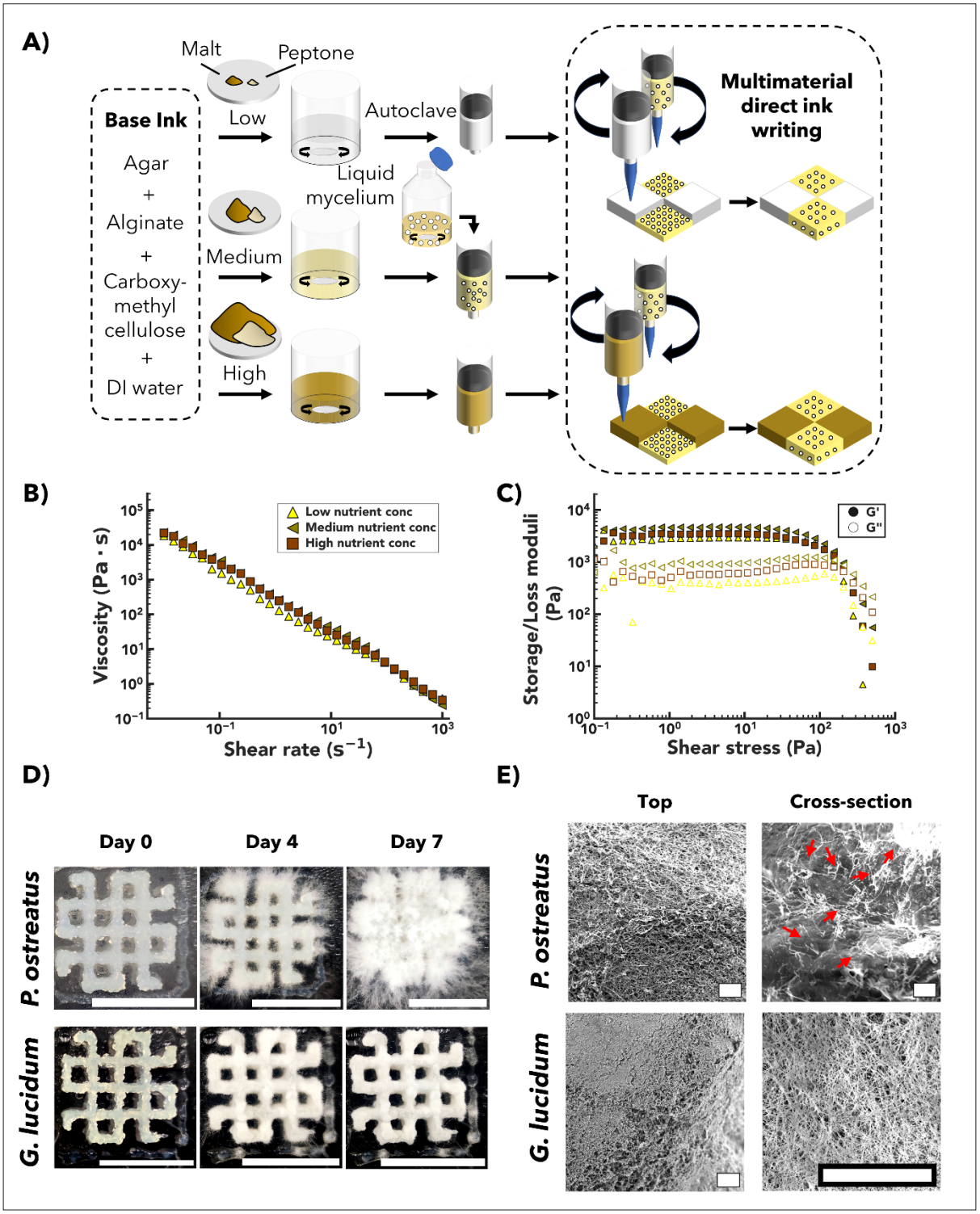

Figure 1. Ink formulation and 3D printing strategies for fungal-based ELMs. (A) Schematics showing the ink preparation with three levels of malt and peptone content (low, medium, high) and the addition of liquid mycelium in the medium-content ink. These inks were then used in the multi-nozzle 3D printer to create materials with local variations in nutrient content and mycelium. (B) Viscosity as a function of shear rate for the inks prepared with the three nutrient levels. (C) Storage (*G*') and loss (*G*") moduli as a function of shear stress for the inks prepared with the three nutrient levels. (D) Digital images of the growth of *G. lucidum* and *P. ostreatus* in 3D-printed constructs over 7 days. Image contrast of all images was slightly enhanced for better clarity. Scale bars: 20 mm. (E) Electron micrographs of the mycelium network of *P. ostreatus* and *G. lucidum* on the top and inside the macropores of 3D-printed constructs after 14 days of growth. Scale bars: 100 μm. For micrographs depicting sparse mycelium networks, red arrows are included to indicate mycelium present.

the structure. Meanwhile, *G. lucidum* was observed to better conform to the 3D-printed structure. Thus, the curves and contours of the 3D structure remained visible even after complete coverage by the mycelium of *G. lucidum*. This observation demonstrates the different foraging strategies that each fungus employs in a similar environment. Furthermore, while *P. ostreatus* readily colonized the air-material surfaces, it had a lower tendency to colonize the cramp spaces within the macropores of the structure. This is shown by the sparse mycelium found in the cross-section of the macropores (Figure 1E). In contrast, the mycelium of *G. lucidum* was equally dense on both the top and inside the macropores of the underlying structure (Figure 1E). However, growth of the mycelium of *P. ostreatus* in the macropores was possible, provided that they are sufficiently large (see Figure S6, Supporting Information).

Having demonstrated the possibility of preparing inks for 3D printing and growing mycelium effectively for two fungal species with different growth behaviors, the effect of the nutrient composition present in the inks on their growth was then studied.

3.2. Nutrient concentration controls the foraging behavior of *P. ostreatus* and *G. lucidum*

Various media and substrates are suitable for fungal cultures. Availability and assay types are among the factors considered when determining the choice of media. Among the plethora of media used for fungal culture, a mixture of malt and peptone are commonly used in the literature and is also chosen here to vary the nutritional content of the inks. Malt serves as a source of polysaccharides to provide energy for the fungi while peptone acts as a nitrogen source for the synthesis of proteins and other components inside the fungal cell. To study the growth of the two fungi *P. ostreatus* and *G. lucidum* when these nutrients are varied, solid-state mycelium growth on agar plates containing low and high levels of malt and peptone were studied (Figure 2, see Figure S7 and time-lapse videos in Videos S1 and S2, Supporting Information).

Agar plates with four levels of nutrient concentrations were prepared following a two-level full factorial design where malt and peptones were varied in low and high concentrations only. The agar plates were inoculated at their center by adding an agar plug containing mycelium. Differences in the mycelium formed from these four nutrient levels could be readily observed for both species (Figure 2A). At low levels of malt and peptone, both *G. lucidum* and *P. ostreatus* formed thin and sparse mycelium. From the naked eye, the mycelium was translucent, with the underlying agar still visible, suggesting it to be very thin and fragile. Increasing the concentration of peptone helped *P. ostreatus* form thicker mycelium, but the mycelium sheet formed was only dense near the inoculating agar plug. The increase growth resulting from the increase in peptone was less pronounced for *G. lucidum*. However, for both strains, malt had a significant effect on the mycelium growth regardless of the concentration of peptone with the mycelium layer becoming opaque at high levels of malt.

To quantify these growth behaviors, the growth rate (the area of mycelium present on the agar plate) was recorded during the 14 days of growth (Figure 2B). Most growth profiles display a sigmoid curve that is typical across different organisms,[40] which was also observed for both fungi in this study. There was an initial lag phase, during which the mycelium from the agar plugs probably initially adjusted to the new environment, followed by an exponential growth phase, and a stationary phase that was reached when the mycelium had covered the entire area of the Petri dish. The growth rate of *P. ostreatus* was faster at low concentrations of malt and peptone as its growth curve was higher than for the other concentrations and was the quickest to plateau (Figure 2B, top). As a fast growth rate is a known attribute of guerrilla-type behavior, this suggests that the fungus adopted an explorative foraging behavior in this environment.[8,22] When the concentration of malt was high, the growth rate became slower but appeared to be independent of the concentration of peptone. The growth rate was the slowest when the concentration of malt was low, and the concentration of peptone was high. Surprisingly, for *G. lucidum*, mycelium grown on agar with high concentrations of malt has a faster rate than those grown on agar with low concentrations of malt (Figure 2B, bottom). This may seem to contradict the theory that low-nutrient environments lead to a faster growth rate due to the fungus exhibiting guerrilla foraging. However, other studies in the literature also suggest that this theory still holds for ranges of malt concentration that are higher than the one used in this study.[8] This suggests that at low malt concentrations, nutrient deficiency may have hindered the growth rate of mycelium. Nevertheless, the mycelium density remained sparser at low-nutrient conditions, which is another attribute indicating guerrilla-type foraging behavior besides high growth rate. Like *P. ostreatus*, the growth rate was the slowest when the concentration of peptone was high while the concentration of malt was low.

To further quantify the exploitative foraging behavior of the fungi, the dry biomass of the mycelium sheet formed in each condition was obtained after 14 days of culture (Figure 2C). At low malt concentrations, an increase in peptone caused a non-significant increase in the thickness of the mycelium formed. Malt had a greater influence on the dry biomass harvested for both strains of fungi investigated

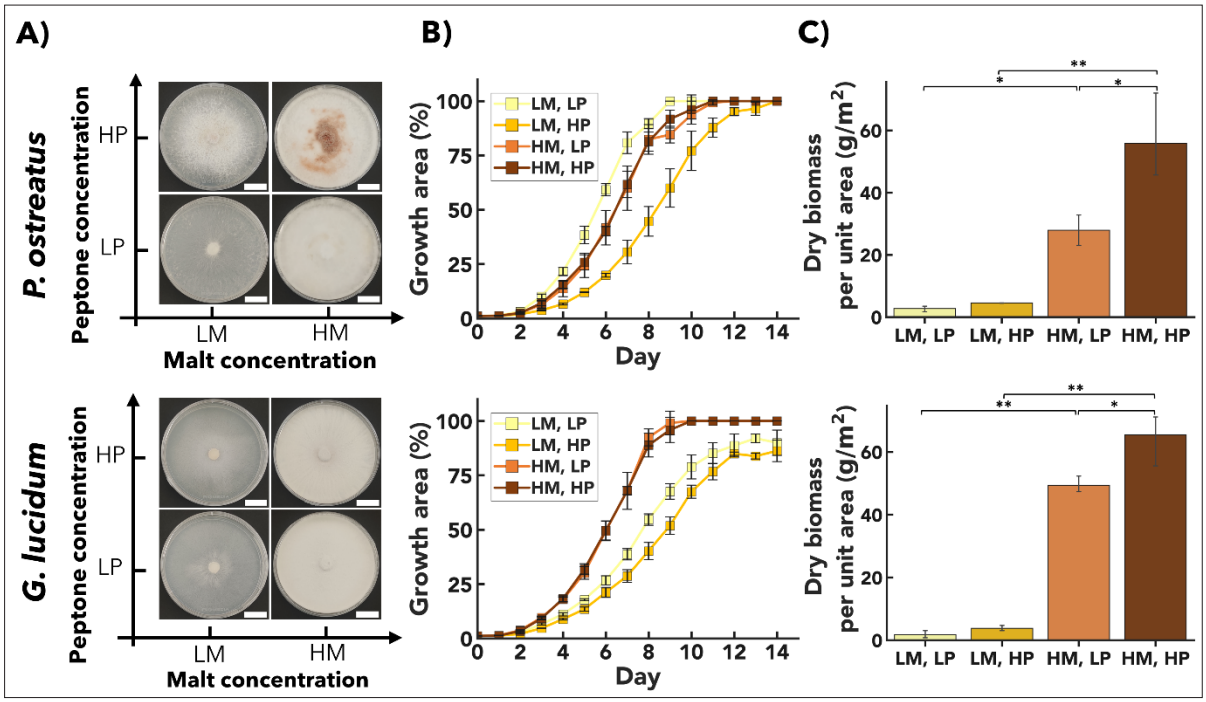

Figure 2. Nutrient concentration controls the foraging behavior of *P. ostreatus* (top panels) and *G. lucidum* (bottom panels). (A) Digital images of mycelium grown on agar plates containing varying concentrations of malt and peptone after 14 days of culture following the two-level full factorial design (see **Materials and methods** section for details). Scale bars: 20 mm. (B) Growth area of the mycelium during 14 days of culture for the four different nutrient compositions. (C) Dry biomass per unit area of the mycelium sheets harvested after 14 days of culture for the four nutrient compositions. Data are presented as mean ± standard deviation. *p <0.05, **p <0.01. Abbreviations: H, high; L, low; M, malt; P, peptone.

but both malt and peptone complemented each other. This synergy resulted in a statistically significant increase in absolute dry biomass obtained when the concentration of peptone was increased at high levels of malt concentration. While malt promoted a greater increase in dry biomass obtained, this quantity increased further in the presence of high levels of peptone.

The variation in malt and peptone concentrations demonstrated various foraging behaviors for the two fungi studied here. This difference in growth led to mycelium formation with differing macroscopic appearances, which could readily influence their properties. A microscopic characterization of the mycelium was therefore conducted to better understand the implications of the varying growth rates.

3.3. Tuning nutrient concentration allows for various morphology of the mycelium of *P. ostreatus* and *G. lucidum*

To determine the effect of the nutrients and the growth rates on the morphology of the mycelium of the two fungi, the mycelium sheets grown in the four nutrient conditions as described in the previous sections were analyzed using electron microscopy (Figure 3).

The microstructures of the mycelium sheets grown after 14 days (Figure 3A) are consistent with the macroscopic observations made from mycelium grown on agar plates (Figure 2A). The density of the mycelium of both *P. ostreatus* and *G. lucidum* increased when the concentration of malt was increased. At low malt and peptone concentrations, there were visible gaps in the network for both strains but as the concentration of nutrients increased, there was tighter packing of the hyphae, owing to the increased mycelium density due to the higher occurrence of branching.

The surface porosity and projected hyphae diameter were also evaluated from these electron micrographs. The surface porosity was significantly reduced when the concentration of malt available to the mycelium increased (Figure 3B). This holds true for both strains regardless of the concentration of peptone. Meanwhile, peptone had a significant influence on the reduction of the surface porosity of the mycelium of *P. ostreatus*, but its effect on the microstructure was negligible for *G. lucidum*. In turn, both malt and peptone had a positive effect on the

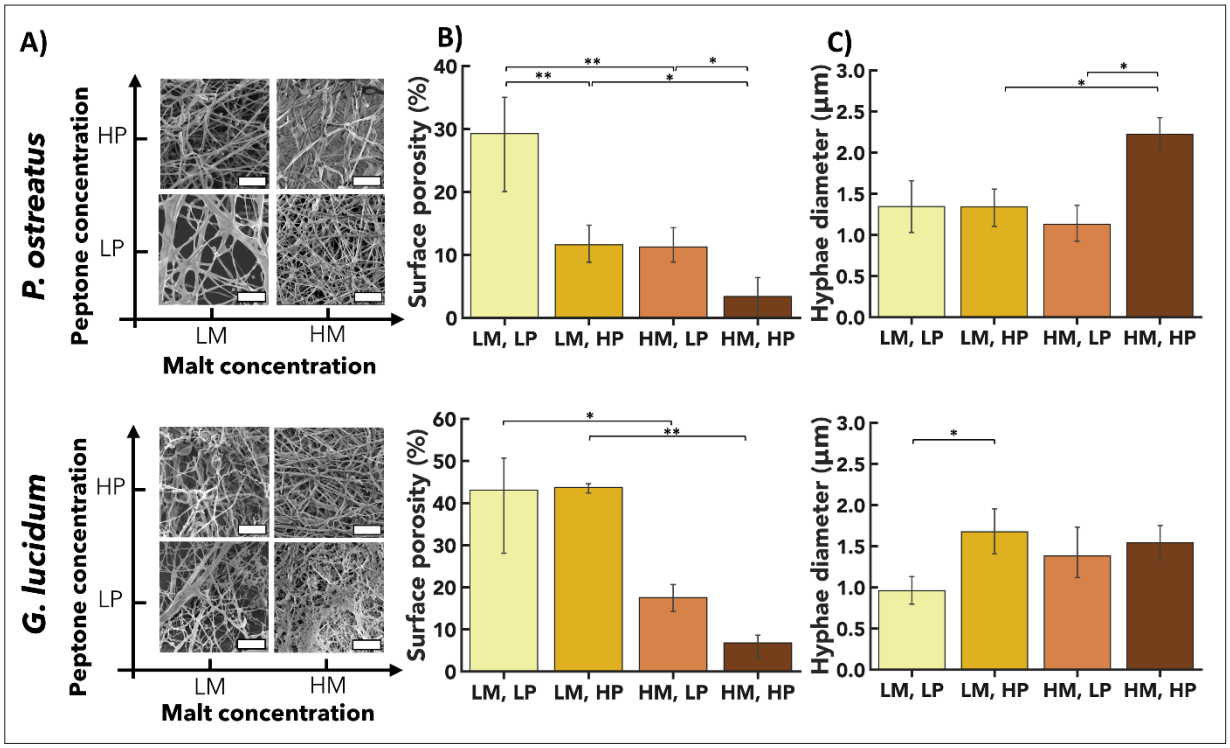

Figure 3. Tuning nutrient concentration allows for various morphology of the mycelium of *P. ostreatus* (top panels) and *G. lucidum* (bottom panels). (A) Electron micrographs of the mycelium grown after 14 days of culture on agar plates containing different concentrations of malt and peptone. Scale bars: 20 µm. (B) Surface porosity of the mycelium after 14 days of culture in the four nutrient conditions. (C) Hyphae diameter of the mycelium after 14 days of culture in the four nutrient conditions. Data are presented as mean ± standard deviation. $^{*}p < 0.05$, $^{**}p < 0.01$. Abbreviations: H, high; L, low; M, malt; P, peptone.

diameter of the hyphae formed that increased when the nutrient concentration increased (Figure 2C). However, the extent of the increase in diameter was different for both strains. For *P. ostreatus*, an increase in malt caused a significant increase in hyphae diameter, but only when the concentration of peptone was high. The same is true for peptone, whereby peptone significantly increased the hyphae diameter when the concentration of malt was high. Meanwhile, for *G. lucidum*, a significant increase in hyphae diameter was observed only when increasing the concentration of peptone when the concentration of malt was low. This observation provides another evidence of the inherent difference between the growth and metabolic activity of both species.

These results establish that malt is more dominant than peptone in affecting the morphology and density of the mycelium of both fungi, resulting in visible macroscopic and microscopic differences. However, peptone by itself still has a significant influence and it cannot be omitted from the formulation of the ink. These macroscopic and microscopic differences may also lead to different surface properties such as hydrophobicity (see Figure S8, Supporting Information). For subsequent experiments on creating structures with localized nutrient variations, low-nutrient zones contained low concentrations of malt and peptone, and high-nutrient zones contained high concentrations of malt and peptone.

3.4. Local variations in nutrients on a two-dimensional surface guide the growth and foraging behavior of mycelium

Considering the difference in growth behaviors of the two fungi on substrates containing different concentrations of nutrients, their behavior on substrates containing local variations in nutrient content was then investigated. To achieve this, multi-material DIW was used to print porous two-dimensional (2D) lattices using the three inks indicated in Figure 1A. The inks were inoculated with liquid mycelium from either *P. ostreatus* or *G. lucidum*, and the fungus was allowed to grow in the structure after printing for about 2 weeks to understand the effects of varying the position of nutrients on the direction of growth and other aspects of the mycelium (Figure 4).

Four sample designs, which could be readily fabricated using our multi-material DIW approach, were tested (Figure 4A). The objective of using these designs was to observe the foraging behavior of mycelium in structures with local variations in nutrient content and to determine if these variations can either promote or inhibit extension (Design I and Design II) or bridging (Design III and Design IV) between different inoculated regions in the structure. Each design contained zones of origin (yellow with white circles), which were printed using the ink containing liquid mycelium and medium levels of malt and peptone. After incubation, the mycelium grew from the zones of origin and extended into the other zones. The prints were intentionally designed to be porous, in order to allow air to flow homogeneously throughout the samples and avoid additional effects of various oxygen contents.

The foraging behavior of the mycelium of *P. ostreatus* on the four structures showed significant variations and effects of the designs (Figure 4B). These results are consistent with the growth of mycelium on various agar formulations (Figure 2), where a clear contrast in mycelium density can be observed between zones of different nutrient levels. When approaching a low-nutrient zone (Design I and Design III), the mycelium formed is sparse. As such, both the extension (Design I) and bridging (Design III) of mycelium are inhibited. This results in a clear contrast between mycelium at the zones of origin and the low-nutrient zones. This contrast

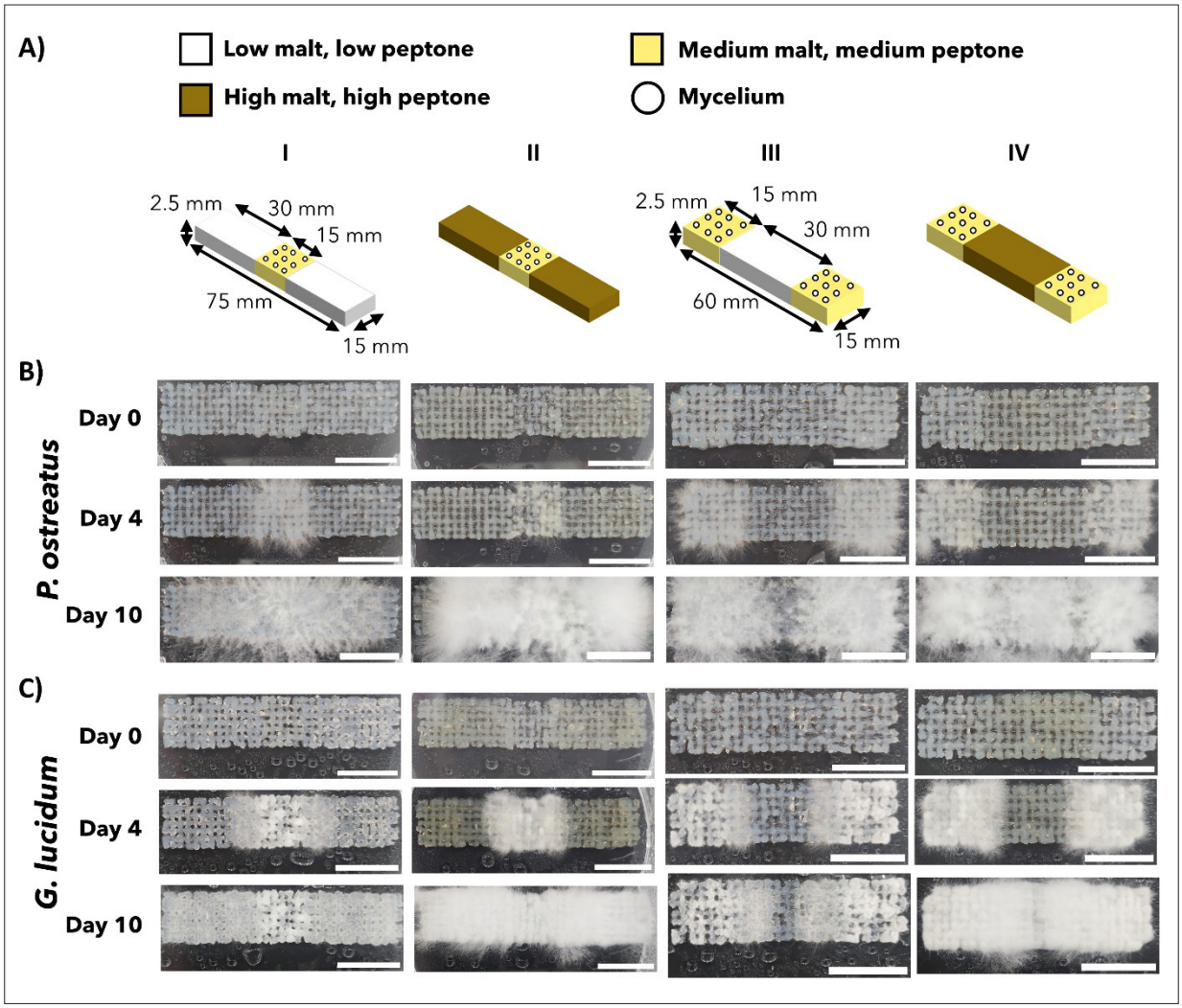

Figure 4. Local variations in nutrients on a 2D surface guides the growth and foraging behavior of mycelium of *P. ostreatus* and *G. lucidum*. (A) Schematics of design of 3D-printed fungal-based engineered living materials (ELMs) detailing the different constituent materials. Growth of mycelium of (B) *P. ostreatus* and (C) *G. lucidum* on the 3D-printed substrates with zones containing varying concentrations of malt, peptone, and liquid mycelium, respectively. Scale bars: 20 mm.

was particularly visible after 4 days of growth and was still apparent after 10 days, albeit less strongly. On the contrary, when the zone had a high nutrient level (Design II and Design IV), both extension and bridging were promoted and the density of mycelium over this zone became indistinguishable from the rest of the network on the ELM. It should be noted, nevertheless, that the extension and bridging are mostly occurring after 10 days. When comparing designs containing high-nutrient zones (Design II and Design IV) to designs containing low-nutrient zones (Design I and Design III), the mycelia emerging from zones of origin were denser for designs containing high-nutrient zones, presumably due to the diffusion of malt and peptone from high-nutrient zones to the zones of origin. For designs with low-nutrient zones, the opposite may also be true, where the initial mycelium formed was sparser due to the diffusion of malt and peptone from the zones of origin to the low-nutrient zones.

Similar observations were made for the same designs containing *G. lucidum* for their extension and bridging in the four multi-material structures (Figure 4C). While the behavior resembled that of *P. ostreatus*, the mycelium of *G. lucidum* had the tendency to conform to the underlying structure with less likelihood to spread its hyphae in all directions, resulting in the shape profile of the underlying structure being more pronounced (compared with Figure 1D). Meanwhile, for *P. ostreatus*, there was also a greater tendency for the mycelium to extend beyond the 3D-printed structure and onto the Petri dish housing the ELM. Otherwise, the growth behavior of both *G. lucidum* and *P. ostreatus* were consistent with the phalanx/guerrilla theory on foraging behavior.

Both Designs I and II also showed the potential of varying local nutrient contents to either promote or inhibit the self-healing capabilities of fungal mycelium. It has been established that live mycelium materials can regenerate,[6,17] allowing holes on mycelium sheets to be filled or two separate structures to combine when placed together. By placing a material of low-nutrient content between two regions containing fungal mycelium, the bridging of mycelium between the two region was inhibited and the self-healing property of the fungal mycelium could be suppressed to a certain extent. Meanwhile, the self-healing capability of mycelium could be promoted if the material in between contained high nutrient levels, promoting the growth of mycelium over the gap. As such, this study also showed the possibility of controlling this phenomenon in fungal-based ELMs.

Therefore, the growth behavior of the two fungi on a flat 2D plane was observed and their behavior in a 3D space was then studied.

3.5. Local variations in nutrients in a 3D complex structure guides the growth and foraging behavior of mycelium

Since ELMs exist in various shapes and complexities, the effects of varying nutrients on all three axes should also be investigated. Furthermore, 3D printing via DIW conveniently allows for 3D shapes to be built and the inks were formulated to allow both extrudability and buildability. The extension and growth of the mycelium from the two species could therefore be observed in three dimensions and in complex patterns (Figure 5).

To test the growth of mycelium in the vertical direction, cuboid structures were designed where the base of the cube is the zone of origin (**Figure 5A**). The structures were again 3D-printed with pores to allow air to flow through the structure and homogeneous growth at the core of the sample. After the base was printed, the subsequent layers were then printed using inks with either a low- or high-nutrient content. For both strains of fungi, the mycelium first emerged from the base of the structure 4 days after printing. However, at this point, the network was barely visible, containing only a few strands of hyphae. By day 7, the mycelium became more visible as the subsequent layers above were gradually covered until complete coverage observed by day 10. If the nutrient content of the higher layers is low, the mycelium formed in the upper layers is sparse, and vice versa. The designs also demonstrated that not all inks used in the fabrication process need to include liquid mycelium. Indeed, only a section needs to be inoculated and the mycelium will eventually envelop the entire structure. This is interesting as it potentially reduces the amount of liquid mycelium required, which should be easier for the fabrication of large-volume structures. It also facilitates the ink preparation and storage as the ink without mycelium can be stored in the fridge until use, whereas inks containing mycelium need to be prepared fresh before use. If an ink containing mycelium is kept for too long, mycelium may develop inside any air bubbles present within the ink, ultimately compromising the homogeneity of the ink leading to 3D printing difficulties later.

From the preceding observations, it has been established that mycelium growth can be controlled through the precise deposition of nutrients in the substrate, allowing for structures with various surface patterns to be fabricated (see also Figures S9 and S10, Supporting Information). As such, a potential application of this technology is the creation of distinct and detailed patterns on the surface of structures. Positioning zones of high- and low-nutrient contents in the ELM should guide the growth of mycelium in specific directions, allowing for the fabrication of structures with esthetical value. Figure 5B highlights an example of this application. Using a low-nutrient zone, the growth of a

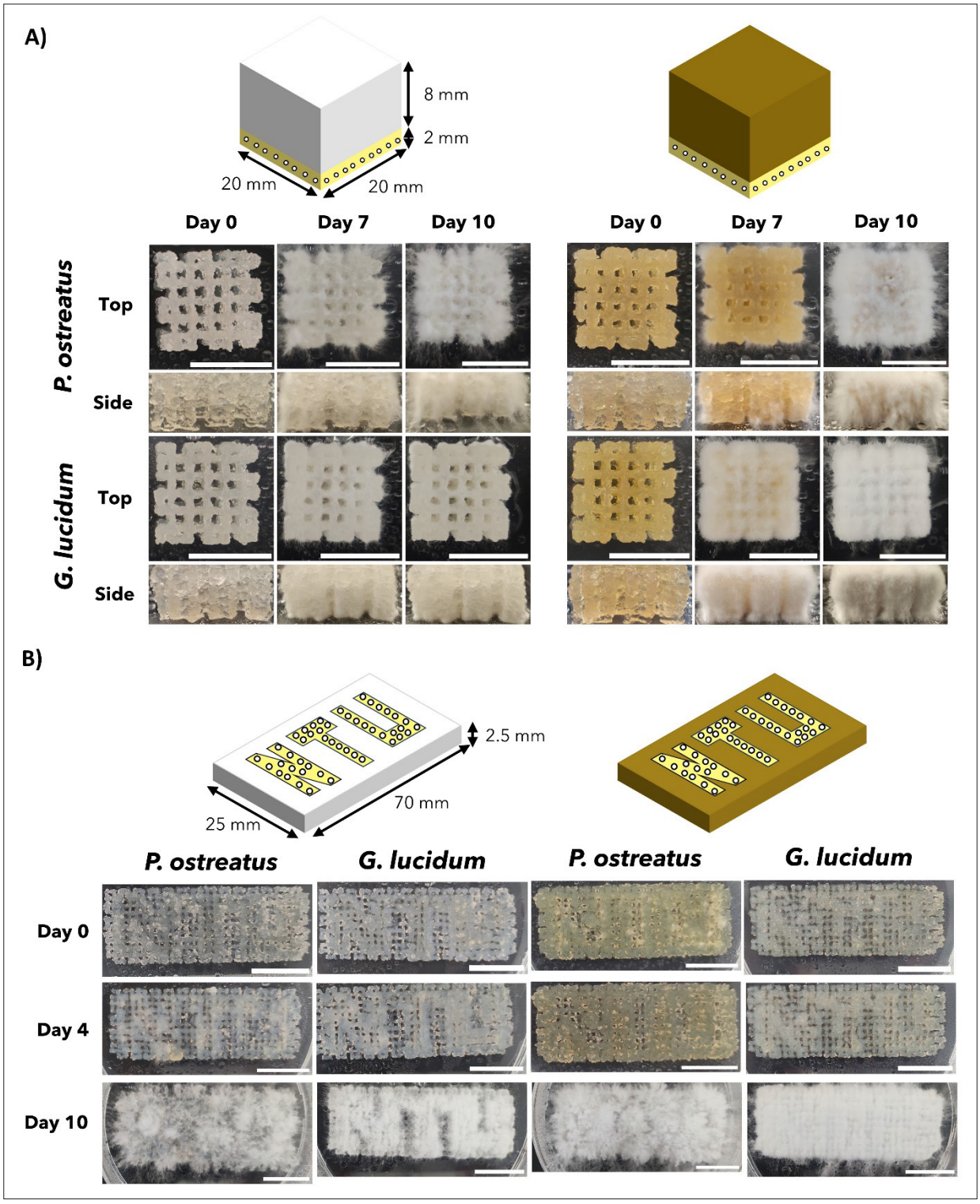

Figure 5. Local variations in nutrients in a 3D complex structure guides the growth and foraging behavior of mycelium from *P. ostreatus* and *G. lucidum*. (A) 3D-printed substrates inoculated with *P. ostreatus* and *G. lucidum*, respectively, with stacked zones containing varying concentrations of malt and peptone. Different fungal strains (*G. lucidum* and *P. ostreatus*) and nutrient contents were used. Scale bars: 20 mm. (B) Fabrication of textured mycelium surfaces by using multi-material 3D printing. Different fungal strains (*G. lucidum* and *P. ostreatus*) and nutrient contents were used. Scale bars: 20 mm.

dense mycelium network was limited to the zones of origin. When the mycelium began to extend into the surrounding low-nutrient level zones, the network became sparser. This creates a contrast in the mycelium network between the two zones, allowing for underlying patterns to be discernible. In contrast, for designs with the surrounding zones containing a high nutrient level, the density of the network was higher, eliminating the underlying pattern of the zone of origin. Owing to the inherent exploitative behavior of *G. lucidum*, pattern generation was more successful when this species was used, with the letterings being distinguishable after attaining complete mycelium growth on day 10. Meanwhile, since it is established that the mycelium of *P. ostreatus* tends to extend in all directions, pattern generation on the surface of the substrate is less successful, despite the visible difference in mycelium density between the high- and low-nutrient zones.

While the effect of nutrient heterogeneity on fungal growth was previously demonstrated in the literature,[21,27,41] this study significantly expands these prior discoveries. Firstly, preceding studies sought to understand fungal growth behavior in soil, and thus, the substrates used were at most 2D. This study does not have such a limitation and therefore also investigates growth in all three spatial dimensions. There is also potential to utilize this knowledge to create fungal-based ELMs and mycelium-bound composites of greater complexity. Regarding the creation of a heterogeneous nutrient environment, previous studies achieved this by manually arranging various cubes of agar to form a tessellation. This study utilizes modern fabrication methods in the form of DIW to fabricate shapes with greater complexity and dimensions, in contrast to those with simple patterns and arrangements. This study also investigates how both factors of the carbon (malt) and nitrogen (peptone) sources interact with each other to affect the growth of fungi on such substrates. On the contrary, previous studies either focused on comparing between different media formulations[21,33,42] or only investigated a single component at a time.[25] Finally, the application of fabricating patterned structures leveraging the ability to manipulate the foraging behavior of fungi was demonstrated in this work, underscoring the potential utility of this phenomenon.

While the use of 3D printing to fabricate fungal-based engineered living materials has been established, notably by the study conducted by Gantenbein et al.,[8] this work seeks to expand on their findings. In this study, instead of a homogenous structure, multi-material samples with heterogeneous distribution of nutrients were fabricated using a multi-nozzle 3D printing system. A second strain of fungi, *P. ostreatus* was explored and the difference in its growth behavior with *G. lucidum* on 3D-printed ELMs in the same environment and with the same nutrient levels was observed as well. This expands on the possibility of different fungi exhibiting different growth patterns on ELMs when generalizing this technology to other strains of fungi. While the difference between explorative and exploitative growth was previously investigated in literature, this was conducted only to optimize the concentration of malt to be included in their final ink composition. In contrast, the nutrient content in the ink used in this study was purposely adjusted to elicit the changes in growth behavior of the mycelium at various locations of the structure. Also, the peptone was included as a second source of nutrients besides malt to determine its main effect on fungal growth and its interaction with malt content.

4. Conclusion

In this study, the effect of different nutrient content on the foraging behavior of mycelium was explored. With two fungal strains used as case studies, their behaviors on multi-material constructs with localized variations in nutrient content fabricated using DIW were investigated. In regions with low-nutrient content, both fungi exhibited guerrilla behavior with mycelium of low density formed, while phalanx behavior was observed in regions of high-nutrient content, resulting in the formation of dense mycelium. *G. lucidum* is more exploitative, with less tendency to extend its hyphae in all directions, as compared to *P. ostreatus*, resulting in greater conformation to the underlying ELM. In the development of existing fungal-based ELMs, this fundamental study provides a possibility of controlling the growth of mycelium on the structure using nutrients to create more complex structures with expanded functionalities. While there was no particular application explored in this study, it is expected that the findings here will provide reference for future developments towards the following applications. Improving the esthetics of apparels made using mycelium is possible by creating patterns containing either high- or low-nutrient content on the surface of such textiles. There is also the potential of using such ELMs as a miniature model of a particular environment to model the behavior of fungi in said environment. This can subsequently be used to better understand the capabilities and effectiveness of using fungi to mycoremediate and remove contaminants from the environment, or to evaluate the efficacy of anti-fungal products. The 3D printing system is also capable of modeling 3D ecosystems with complex shapes and is not limited to just creating a 2D ecosystem.

Beyond the investigation of malt and peptone, other nutrient sources can also be explored as well. The effect of other materials on the growth and foraging behavior of mycelium such as metal ions and other microorganisms

including bacteria and plant cells can also be incorporated and investigated, provided that the printability of the ink is not affected by the incorporation of such materials. Fungal behavior in complex architectures manufactured via 3D printing can also be another potential area inspired by this study, opening the way for the exploration of 3D-printed biodegradable and living products.

Acknowledgements

None.

Funding

The authors acknowledge funding from the National Research Foundation of Singapore and ETH Zurich, Switzerland, with the grant Future Cities Laboratory Global, Module A4: Mycelium digitalization.

Conflict of interest

The authors declare they have no competing interests.

Author contributions

Conceptualization: Jia Heng Teoh, Hortense Le Ferrand
Formal analysis: Jia Heng Teoh
Funding acquisition: Hortense Le Ferrand
Investigation: Jia Heng Teoh
Methodology: Jia Heng Teoh, Eugene Soh
Supervision: Hortense Le Ferrand
Visualization: Jia Heng Teoh, Hortense Le Ferrand
Writing – original draft: Jia Heng Teoh
Writing – review & editing: All authors

Ethics approval and consent to participate

Not applicable.

Consent for publication

Not applicable.

Availability of data

Additional data are available in the Supplementary File. Data are available from the corresponding author upon reasonable request.

References

1. Rodrigo-Navarro A, Sankaran S, Dalby MJ, del Campo A, Salmeron-Sanchez M. Engineered living biomaterials. *Nat Rev Mater*. 2021;6(12):1175-1190.
doi: 10.1038/s41578-021-00350-8

2. Wang Y, Liu Y, Li J, Chen Y, Liu S, Zhong C. Engineered living materials (ELMs) design: from function allocation to dynamic behavior modulation. *Curr Opin Chem Biol*. 2022;70:102188.
doi: 10.1016/j.cbpa.2022.102188

3. Lantada AD, Korvink JG, Islam M. Taxonomy for engineered living materials. *Cell Rep Phys Sci*. 2022;3(4):100807.
doi: 10.1016/j.xcrp.2022.100807

4. Vandelook S, Elsacker E, Van Wylick A, De Laet L, Peeters E. Current state and future prospects of pure mycelium materials. *Fungal Biol Biotechnol*. 2021;8(1):20.
doi: 10.1186/s40694-021-00128-1

5. Jones M, Gandia A, John S, Bismarck A. Leather-like material biofabrication using fungi. *Nat Sustain*. 2021;4(1):9-16.
doi: 10.1038/s41893-020-00606-1

6. Elsacker E, Zhang M, Dade-Robertson M. Fungal engineered living materials: the viability of pure mycelium materials with self-healing functionalities. *Adv Funct Mater*. 2023;33(29):2301875.
doi: 10.1002/adfm.202301875

7. McBee RM, Lucht M, Mukhitov N, et al. Engineering living and regenerative fungal–bacterial biocomposite structures. *Nat Mater*. 2022;21(4):471-478.
doi: 10.1038/s41563-021-01123-y

8. Gantenbein S, Colucci E, Käch J, et al. Three-dimensional printing of mycelium hydrogels into living complex materials. *Nat Mater*. 2023;22(1):128-134.
doi: 10.1038/s41563-022-01429-5

9. Brand A, Gow NA. Mechanisms of hypha orientation of fungi. *Curr Opin Microbiol*. 2009;12(4):350-357.
doi: 10.1016/j.mib.2009.05.007

10. Soh E, Le Ferrand H. Woodpile structural designs to increase the stiffness of mycelium-bound composites. *Mater Design*. 2023;225:111530.
doi: 10.1016/j.matdes.2022.111530

11. Murphy SV, Atala A. 3D bioprinting of tissues and organs. *Nat Biotechnol*. 2014;32(8):773-785.
doi: 10.1038/nbt.2958

12. Schaffner M, Rühs PA, Coulter F, Kilcher S, Studart AR. 3D printing of bacteria into functional complex materials. *Sci Adv*. 2017;3(12):eaao6804.
doi: 10.1126/sciadv.aao6804

13. Teoh JH, Mozhi A, Sunil V, Tay SM, Fuh J, Wang CH. 3D printing personalized, photocrosslinkable hydrogel wound dressings for the treatment of thermal burns. *Adv Funct Mater*. 2021;31(48):2105932.
doi: 10.1002/adfm.202105932

14. Skylar-Scott MA, Mueller J, Visser CW, Lewis JA. Voxelated soft matter via multimaterial multinozzle 3D printing. *Nature*. 2019;575(7782):330-335.
doi: 10.1038/s41586-019-1736-8

15. Cheng J, Wang R, Sun Z, et al. Centrifugal multimaterial 3D printing of multifunctional heterogeneous objects. *Nat Commun*. 2022;13(1):1-10.

doi: 10.1038/s41467-022-35622-6

16. Soh E, Chew ZY, Saeidi N, Javadian A, Hebel D, Le Ferrand H. Development of an extrudable paste to build mycelium-bound composites. *Mater Design*. 2020;195:109058. doi: 10.1016/j.matdes.2020.109058
17. Soh E, Teoh JH, Leong B, Xing T, Le Ferrand H. 3D printing of mycelium engineered living materials using a waste-based ink and non-sterile conditions. *Mater Design*. 2023;236:112481. doi: 10.1016/j.matdes.2023.112481
18. Elsacker E, Peeters E, De Laet L. Large-scale robotic extrusion-based additive manufacturing with living mycelium materials. *Sustain Fut*. 2022;4:100085. doi: 10.1016/j.sftr.2022.100085
19. Jauk J, Gosch L, Vašatko H, Christian I, Klaus A, Stavric M. MyCera. Application of mycelial growth within digitally manufactured clay structures. *Int J Arch Comput*. 2022;20(1):147807712210822. doi: 10.1177/14780771221082248
20. Shen SC, Lee NA, Lockett WJ, et al. Robust myco-composites: a biocomposite platform for versatile hybrid-living materials. *Mater Horiz*. 2024;11(7):1689-1703. doi: 10.1039/D3MH01277H
21. Boswell GP, Jacobs H, Davidson FA, Gadd GM, Ritz K. Functional consequences of nutrient translocation in mycelial fungi. *J Theor Biol*. 2002;217(4):459-477. doi: 10.1006/jtbi.2002.3048
22. Aleklett K, Ohlsson P, Bengtsson M, Hammer EC. Fungal foraging behaviour and hyphal space exploration in micro-structured Soil Chips. *ISME J*. 2021;15(6):1782-1793. doi: 10.1038/s41396-020-00886-7
23. Ye XH, Yu FH, Dong M. A trade-off between guerrilla and phalanx growth forms in *Leymus secalinus* under different nutrient supplies. *Ann Bot*. 2006;98(1):187-191. doi: 10.1093/aob/mcl086
24. Fomina M, Ritz K, Gadd GM. Nutritional influence on the ability of fungal mycelia to penetrate toxic metal-containing domains. *Mycol Res*. 2003;107(7):861-871. doi: 10.1017/S095375620300786X
25. Nussbaum N, von Wyl T, Gandia A, Romanens E, Rühs PA, Fischer P. Impact of malt concentration in solid substrate on mycelial growth and network connectivity in Ganoderma species. *Sci Rep*. 2023;13(1):21051. doi: 10.1038/s41598-023-48203-4
26. Fukasawa Y, Ishii K. Foraging strategies of fungal mycelial networks: responses to quantity and distance of new resources. *Front Cell Dev Biol*. 2023;11:1244673. doi: 10.3389/fcell.2023.1244673
27. Davidson FA, Park AW. A mathematical model for fungal development in heterogeneous environments. *Appl Math Lett*. 1998;11(6):51-56. doi: 10.1016/S0893-9659(98)00102-5
28. Aguilar-Trigueros CA, Boddy L, Rillig MC, Fricker MD. Network traits predict ecological strategies in fungi. *ISME Commun*. 2022;2(1):1-11. doi: 10.1038/s43705-021-00085-1
29. Veresoglou SD, Wang D, Andrade-Linares DR, Hempel S, Rillig MC. Fungal decision to exploit or explore depends on growth rate. *Microb Ecol*. 2018;75(2):289-292. doi: 10.1007/s00248-017-1053-4
30. Schneider CA, Rasband WS, Eliceiri KW. NIH image to ImageJ: 25 years of image analysis. *Nat Methods*. 2012;9(7):671-675. doi: 10.1038/nmeth.2089
31. Yang L, Park D, Qin Z. Material function of mycelium-based bio-composite: a review. *Front Mater*. 2021;8:737377. doi: 10.3389/fmats.2021.737377
32. Hotz EC, Bradshaw AJ, Elliott C, Carlson K, Dentinger BTM, Naleway SE. Effect of agar concentration on structure and physiology of fungal hyphal systems. *J Mater Res Technol*. 2023;24:7614-7623. doi: 10.1016/j.jmrt.2023.05.013
33. Hoa HT, Wang CL. The effects of temperature and nutritional conditions on mycelium growth of two oyster mushrooms (*Pleurotus ostreatus* and *Pleurotus cystidiosus*). *Mycobiology*. 2015;43(1):14-23. doi: 10.5941/MYCO.2015.43.1.14
34. Qiu Z, Wu X, Gao W, Zhang J, Huang C. High temperature induced disruption of the cell wall integrity and structure in Pleurotus ostreatus mycelia. *Appl Microbiol Biotechnol*. 2018;102(15):6627-6636. doi: 10.1007/s00253-018-9090-6
35. Wang J, Liu Y, Zhang X, et al. 3D printed agar/ calcium alginate hydrogels with high shape fidelity and tailorable mechanical properties. *Polymer*. 2021;214:123238. doi: 10.1016/j.polymer.2020.123238
36. Mallakpour S, Azadi E, Hussain CM. State-of-the-art of 3D printing technology of alginate-based hydrogels—an emerging technique for industrial applications. *Adv Colloid Interface Sci*. 2021;293:102436. doi: 10.1016/j.cis.2021.102436
37. Jones EBG, Jennings DH. The effect of cations on the growth of fungi. *New Phytol*. 1965;64(1):86-100. doi: 10.1111/j.1469-8137.1965.tb05378.x
38. Lin N, Taghizadehmakoei A, Polovina L, et al. 3D bioprinting of food grade hydrogel infused with living *Pleurotus ostreatus* Mycelium in non-sterile conditions. *ACS Appl Bio Mater*. 2024;7(5):2982-2992. doi: 10.1021/acsabm.4c00048
39. Abdallah YK, Estévez AT. Biowelding 3D-Printed biodigital brick of seashell-based biocomposite by pleurotus ostreatus mycelium. *Biomimetics*. 2023;8(6):504. doi: 10.3390/biomimetics8060504

40. Kaufmann KW. Fitting and using growth curves. *Oecologia*. 1981;49(3):293-299. doi: 10.1007/BF00347588

41. Ritz K. Growth responses of some soil fungi to spatially heterogeneous nutrients. *FEMS Microbiol Ecol*. 1995;16(4):269-279. doi: 10.1111/j.1574-6941.1995.tb00291.x

42. Haneef M, Ceseracciu L, Canale C, Bayer IS, Heredia-Guerrero JA, Athanassiou A. Advanced materials from fungal mycelium: fabrication and tuning of physical properties. *Sci Rep*. 2017;7(1):41292. doi: 10.1038/srep41292